# Preparation of π-Conjugated Poly(thiophene-2,5-diyl), Poly(p-phenylene), and Related Polymers Using Zerovalent Nickel Complexes. Linear Structure and Properties of the π-Conjugated Polymers

**Takakazu Yamamoto,* Atsushi Morita, Yuichi Miyazaki, Tsukasa Maruyama, Hiroshi Wakayama, Zhen-hua Zhou, Yoshiyuki Nakamura, and Takaki Kanbara**

*Research Laboratory of Resources Utilization, Tokyo Institute of Technology, 4259 Nagatsuta, Midori-ku, Yokohama 227, Japan*

**Shintaro Sasaki**

*Department of Polymer Science, Tokyo Institute of Technology, 2-12-1, Ookayama, Meguro, Tokyo 152, Japan*

**Kenji Kubota**

*Gumma University, Tenjincho, Kiryui 376, Japan*

*Received July 12, 1991; Revised Manuscript Received October 1, 1991*

ABSTRACT: Dehalogenation polycondensation of 2,5-dihalothiophene, 2,5-dihalo-3-alkylthiophene, and 1,4-dihalobenzene with zerovalent nickel complexes, typically a mixture of bis(1,5-cyclooctadiene)nickel(0) ($Ni(cod)_2$) and neutral ligand L (e.g., $PPh_3$), affords π-conjugated poly(thiophene-2,5-diyl) (PTh), poly(3-alkylthiophene-2,5-diyl) (PRTh), and poly(p-phenylene) (PPP), respectively, in high yields at 25–100 °C. Analogous dehalogenation of 2,5-dibromo-3-cyanothiophene, 4,4′-dibromobiphenyl, and 2,7-dibromo-9,10-dihydrophenanthrene also affords the corresponding π-conjugated aromatic polymers. PRTh contains head-to-head junctions in high content (ca. 60%) and has a molecular weight of 15 000–190 000. Powder X-ray diffraction patterns of PTh and PPP indicate that they have high crystallinity. Vacuum deposition of PTh and PPP on substrates (carbon, gold, and aluminum) gives crystalline thin films where the polymer molecules are arranged perpendicularly to the surface of the substrates as proved by electron diffraction patterns of the vacuum-deposited film. PRTh adopts a random-coil structure in $CHCl_3$ and shows a large specific refractive index increment ($\Delta n/\Delta c = 0.35\ cm^3\ g^{-1}$). Doping of PTh with iodine and $FeCl_3$ affords electrically conducting materials with an electrical conductivity of $10^0$–$10^{1.5}$ S $cm^{-1}$ as measured with pellets obtained from powder samples. The iodine-doped PTh can be completely undoped with hydrazine to recover neutral PTh. The iodine-doped PTh forms a new one-dimensional structure with a spacing of 1.0 nm.

## Introduction

Diorganonickel(II) complexes $NiR_2L_n$ undergo a reductive coupling reaction to give R–R[1,2] (eq 1), and this

$$L_nNiR_2 \rightarrow R\text{–}R \quad (1)$$

coupling reaction has been utilized to carry out nickel-catalyzed C–C coupling between Grignard reagent and organic halide (eq 2)[3] and dehalogenation coupling of organic halides with zinc (eq 3).[4] In addition to the

$$RMgX + R'X \rightarrow R\text{–}R' + MgX_2 \quad (2)$$

$$2RX + Zn \rightarrow R\text{–}R + ZnX_2 \quad (3)$$

coupling reactions expressed by eqs 2 and 3, Ullmann type coupling of organic halides using zerovalent nickel complex itself as a dehalogenation reagent[5] has been developed.

$$2RX + NiL_n \rightarrow R\text{–}R + NiX_2L_n \quad (4)$$

Among these organonickel-based coupling reactions, reactions 2 and 3 have been developed for molecular design of electrically conducting π-conjugated poly(arylene)s $-(Ar)_n-$, e.g., linear poly(p-phenylene),[6] poly(thiophene-2,5-diyl)[7] and its alkyl derivatives,[7d,8] poly(N-alkylpyrrole-2,5-diyl),[9] and poly(ferrocene-1,1′-diyl).[10]

$$nX\text{–}Ar\text{–}X + nMg\ (\text{or } Zn) \xrightarrow{\text{Ni complex}} -(Ar)_n- \quad (5)$$

However, much less attention has been paid[11] to application of coupling reaction 4 to the synthesis of the π-conjugated polymer.

Since coupling reaction 4 proceeds under mild conditions, can be applied to a wide range of aromatic compounds (e.g., those with carbonyl and cyano groups) under various reaction conditions (e.g., in various solvents), and is the most direct and simple reaction among the Ni-based coupling reactions, reaction 4 is expected to provide a versatile means for molecular design and synthesis of electrically conducting π-conjugated polymers from dihaloaromatic compounds X–Ar–X.

$$nX\text{–}Ar\text{–}X + nNiL_m \rightarrow -(Ar)_n- + nNiX_2L_m \quad (6)$$

We now report results of the application of the coupling reaction to the preparation of typical π-conjugated poly(arylene)s, poly(p-phenylene), poly(thiophene-2,5-diyl), poly(3-alkylthiophene-2,5-diyl), and related polymers.

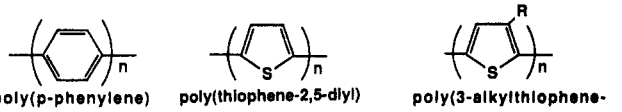


poly(p-phenylene) PPP — poly(thiophene-2,5-diyl) PTh — poly(3-alkylthiophene-2,5-diyl) PRTh

The new polymerization has been found to afford π-conjugated polymers with well-defined linkage between the monomer units and to be suited to the investigation of the crystal structure and the doping process of the polymers. Recently, several other organometallic pro-

0024-9297/92/2225-1214$03.00/0 

**Table I**
**Preparation of Poly(thiophene-2,5-diyl), Poly(*p*-phenylene), and Related Polymers by Dehalogenation Polycondensation of X-Ar-X with a Mixture of $Ni(cod)_2$ and Neutral Ligand L**

| run | monomer (X-Ar-X)[a] (concn, M) | ligand[b] | reaction conditions: solvent | temp, °C | time, h | yield,[c] % | mol wt[d]: $M_n$ | $M_w$ |
|---|---|---|---|---|---|---|---|---|
| 1 | 2,5-$Br_2$-Th (0.25) | $PPh_3$ | DMF | 100 | 16 | 92 | | |
| 2 | 2,5-$Br_2$-Th (0.25) | $PPh_3$ | DMF | 80 | 16 | 100 | | |
| 3 | 2,5-$Br_2$-Th (0.25) | $PPh_3$ | DMF | 60 | 16 | 100 | | |
| 4 | 2,5-$Br_2$-Th (0.25) | $PPh_3$ | DMF | 40 | 16 | 80 | | |
| 5 | 2,5-$Br_2$-Th (0.25) | $PPh_3$ | DMF | 25 | 24 | 74 | | |
| 6 | 2,5-$Br_2$-Th (0.25) | $PPh_3$ | DMF | 60 | 2 | 100 | | |
| 7 | 2,5-$Br_2$-Th (0.25) | $Ni(PPh_3)_4$[e] | DMF | 60 | 16 | 63 | | |
| 8 | 2,5-$Br_2$-Th (0.25) | bpy | DMF | 60 | 16 | 91 | | |
| 9 | 2,5-$Br_2$-Th (0.25) | bpy | DMF | 25 | 24 | 93 | | |
| 10 | 2,5-$Cl_2$-Th (0.25) | $PPh_3$ | DMF | 60 | 16 | 55 | | |
| 11 | 2,5-$Br_2$-3MeTh (0.25) | $PPh_3$ | DMF | 60 | 16 | 76 | | |
| 12 | 2,5-$I_2$-3HexTh (0.13) | $PPh_3$ | DMF | 60 | 48 | 60 | | |
| 13 | 2,5-$I_2$-3HexTh (0.25) | bpy | DMF | 60 | 16 | 70 | (7400) | 52000 (30300) |
| 14 | 2,5-$I_2$-3HexTh (0.13) | bpy | DMF | 60 | 48 | 94 | | 190000 |
| 15 | 2,5-$I_2$-3HexTh (0.18) | bpy | toluene | 60 | 48 | 60 | | |
| 16 | 2,5-$I_2$-3OctTh (0.13) | bpy | DMF | 60 | 48 | 80 | | |
| 17 | 2,5-$I_2$-3OctTh (0.13) | bpy | DMF | 30 | 48 | 80 | (15000) | (23000) |
| 18 | 2,5-$I_2$-3DodTh (0.13) | bpy | DMF | 60 | 48 | 87 | | |
| 19 | 3,5-$Br_2$-3CNTh (0.25) | $PPh_3$ | DMF | 60 | 16 | 91 | | |
| 20 | 2,5-$Br_2$-3CNTh (0.25) | bpy | DMF | 25 | 48 | 80 | | |
| 21 | 1,4-$Br_2$-Ben (0.20) | $PPh_3$ | DMF | 60 | 16 | 26 | | |
| 22 | 1,4-$Br_2$-Ben (0.20) | bpy | DMF | 60 | 16 | 99 | | |
| 23 | 1,4-$Br_2$-Ben (0.20) | bpy | DMF | 30 | 24 | 95 | | |
| 24 | 1,4-$I_2$-Ben (0.20) | bpy | DMF | 60 | 16 | 91 | | |
| 25 | 1,4-$Cl_2$-Ben (0.20) | bpy | DMF | 60 | 16 | 92 | | |
| 26 | 4,4'-$Br_2$-diBen (0.20) | bpy | DMF | 60 | 48 | 95 | | |
| 27 | 9,10-$X_2$-Anth (0.10) | $PPh_3$ | THF | 60 | 8 | 0 (complex) | | |
| 28 | 2,7-$Br_2$-9,10-$H_2$Phen (0.13) | bpy | DMF | 60 | 24 | 90 | | |

[a] 2,5-$X_2$-Th = 2,5-dihalothiophene, 2,5-$I_2$-3RTh = 2,5-diiodo-3-alkylthiophene (R: Hex = hexyl, Oct = octyl, Dod = dodecyl), 2,5-$Br_2$-CNTh = 2,5-dibromo-3-cyanothiophene, 1,4-$X_2$-Ben = 1,4-dihalobenzene, 2,7-$Br_2$-9,10-$H_2$Phen = 2,7-dibromo-9,10-dihydrophenanthrene. [b] $PPh_3$ = triphenylphosphine, bpy = 2,2'-bipyridyl. [c] Yield was calculated based on carbon recovered: (% carbon in polymer) × (weight of polymer)/(weight of carbon in monomer). [d] $M_n$ = number-average molecular weight, $M_w$ = weight-average molecular weight. Values without parentheses were determined by the light scattering method, whereas values in parentheses were determined by gel permeation chromatography (GPC). [e] $Ni(PPh_3)_4$ was used instead of the mixture of $Ni(cod)_2$ and L.

cesses were reported to be suitable for the preparation of π-conjugated polymers.[12]

## Results and Discussion

**Homopolymerization.** Polycondensation of the following dihalo organic compounds has been carried out.

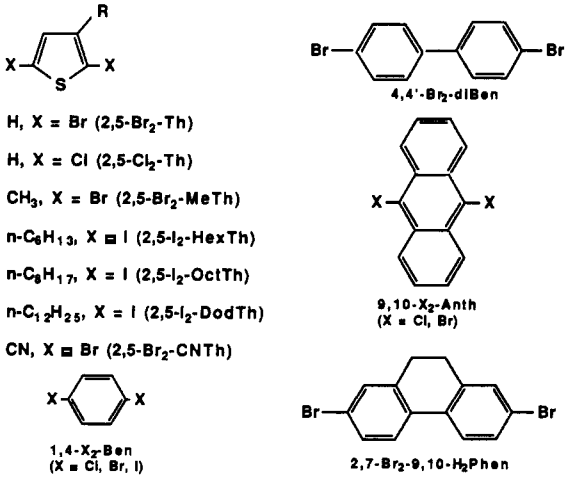


Table I summarizes results of polymerization of 2,5-dihalothiophene, 1,4-dibromobenzene, and the related monomers. As the dehalogenating Ni(0) complex, mixtures of bis(1,5-cyclooctadiene)nickel ($Ni(cod)_2$) and neutral ligand L were mainly employed.

As shown in runs 1–6 in Table I, the dehalogenation polycondensation of 2,5-$Br_2$-Th with a mixture of $Ni(cod)_2$ and $PPh_3$ proceeds smoothly in the temperature range 25–100 °C. On mixing 2,5-$Br_2$-Th with the Ni(0) complex, precipitation of a reddish brown polymer starts immediately, and the best yield is attained at 60–80 °C. The polymer obtained has the following π-conjugated PTh structure as revealed by its analytical data and comparison of its IR spectrum with that of previously reported PTh.[7]

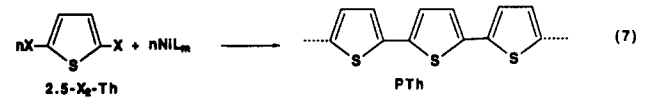


(7)

Most of the obtained PTh was unextractable by hot $CHCl_3$, indicating that most of the PTh had a molecular weight higher than 3000.[7i] Even at short polymerization time (2 h, run 6), an almost quantitative yield is attained. However, PTh obtained at short polymerization time contained a relatively high content of Br (3.9%), and the content of Br decreased to 1.8% (at 8 h at 60 °C) and 0.7% (at 16 h at 60 °C, run 3) with increasing polymerization time, revealing that chain growth by coupling of the seemingly insoluble precipitate of PTh having a terminal C-Br bond proceeded even after formation of the precipitate. The $CHCl_3$-extractable fraction of PTh decreased from 3.2% to 1.2% with increasing polymerization time from 2 to 16 h at 60 °C.

$Ni(PPh_3)_4$ also affords PTh (run 7); however, the yield is lower, indicating that the coordinatively saturated Ni-

$(PPh_3)_4$ has a lower reactivity compared with the mixture of $Ni(cod)_2$ and $PPh_3$. Use of bpy instead of $PPh_3$ affords similar results (runs 8 and 9). 2,5-$Cl_2$-Th shows a lower reactivity than 2,5-$Br_2$-Th and affords a lower yield (run 10). The CP-MAS $^{13}C$-NMR spectrum of the present PTh (solid) shows peaks at 136 and 125 ppm assigned to the 2,5 carbons and the 3,4 carbons, respectively, and no other peak was observable.

Polymerization of 2,5-dihalo-3-alkylthiophenes, 2,5-$X_2$-RTh (R = $CH_3$, $n$-$C_6H_{13}$, $n$-$C_8H_{17}$, $n$-$C_{12}H_{25}$), gives the corresponding soluble poly(3-alkylthiophene-2,5-diyl)s (PRTh's),[8] which, in spite of the sterically large R groups, are considered to have a $\pi$-conjugation system similar to that of PTh as judged from their reddish brown color and electrically conducting property.[7d,8a,b]

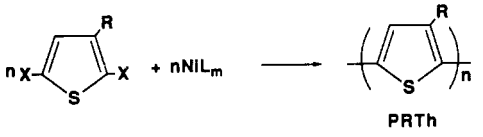

(8)

PRTh has been prepared by reaction 5,[7d,8] oxidation of 3-alkylthiophene,[13] and electrochemical polymerization.[14] Comparison of the $^1H$-NMR spectra[14e] of the variously prepared PRTh's reveals that the content of head-to-head junctions in PRTh's prepared by the organometallic

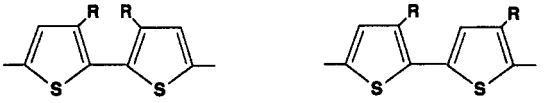


technique (the present method and the method expressed by eq 5[7d,8]) is considerably higher (ca. 60–70%) than that (ca. 10%) in PRTh's prepared by oxidation and electrochemical polymerization. In the $^1H$-NMR spectrum of the present PRTh, the peak of the thiophene ring-attached-$CH_2$ proton ($\delta$ 2.55)[14e] of the head-to-head unit is stronger than that ($\delta$ 2.8) of the head-to-tail unit.

The high content of the head-to-head unit in PRTh prepared by the organometallic technique suggests the organometallic coupling reactions (eqs 2–4) proceed with some regioselectivity; presumably the following 4,4'-dialkyl-5,5'-dihalo-2,2'-bithiophene is the major species formed in the initial step of the polycondensation.

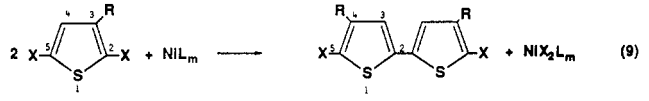

(9)

Easier oxidative addition of the 5-C–X bond to the Ni(0) complex than that of the 2-C–X bond because of the steric effect of R explains the major formation of the symmetrical bithiophene derivative shown above and thus elucidates the high content of the head-to-head junctions in PRTh. Increase in polymerization time (cf. runs 13 and 14 in Table I) leads to an increase of molecular weight of poly(3-hexylthiophene-2,5-diyl). The weight-average molecular weight ($M_w$) of PRTh determined by light scattering roughly agrees with that determined by GPC (polystyrene standard; cf. run 13). PRTh shows a $\pi$–$\pi^*$ absorption band at 380–400 nm in $CHCl_3$. Both PTh and PRTh have good thermal stability; TGA under $N_2$ shows a residual weight of 80% at 600 °C and 81% at 400 °C for PTh and PRTh (R = $n$-$C_{12}H_{25}$), respectively. Polymerization of 2,5-$Br_2$-CNTh (runs 19 and 20) gives the corresponding poly(3-cyanothiophene-2,5-diyl), whose IR spectrum shows a $\nu$(C≡N) vibration at 2230 $cm^{-1}$. This polymer is sparingly soluble in organic solvents.

Polymerization of 1,4-$X_2$-Ben and 4,4'-$Br_2$-diBen affords yellow and fluorescent PPP in high yields when it is carried out in the presence of bpy (runs 22–26). However, carrying out the polymerization in the presence of $PPh_3$ (run 21) affords PPP in only low yield. The difference between the two polymerizations may be attributed to the difference in the configuration of intermediate nickel(II) complexes formed by using bpy and $PPh_3$. The polymerization is now assumed to proceed through oxidative addition of 1,4-$X_2$-Ben to the Ni(0) complex to form (4-halophenyl)-halonickel(II) complex $L_mNiX(C_6H_4X)$, disproportionation of $L_mNiX(C_6H_4X)$ to afford bis(4-halophenyl)nickel-(II) complex $L_mNi(C_6H_4X)_2$, and reductive elimination of $XC_6H_4C_6H_4X$ from $L_mNi(C_6H_4X)_2$. The propagation process involving coupling between $X(C_6H_4)_xX$ and $X(C_6H_4)_yX$ is also accounted for by similar basic reactions.

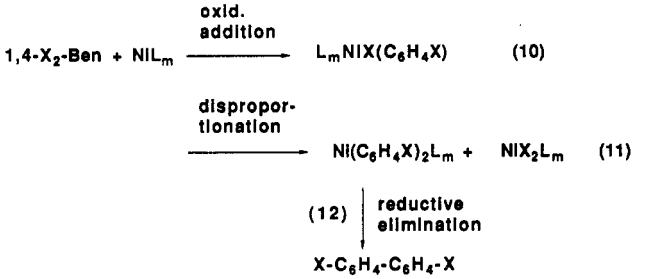


Such basic reactions as shown in eqs 10 and 11 are well established in organometallic chemistry,[1,2] and it is known that tertiary phosphine ligands such as $PPh_3$ usually afford trans-Ni(II) complex[15] whereas the bidentate bpy ligand definitely affords cis-Ni(II) complex. The reductive elimination usually proceeds more easily in the cis-type complex than in the trans-type complex,[1,2,16] and the disproportionation reaction involving exchange of the anionic ligands X and $C_6H_4X$ (eq 11) also may proceed more easily in the cis-type complex.

In the case of 9,10-$X_2$-Anth (run 27), its reaction with a mixture of $Ni(cod)_2$ and $PPh_3$ affords a complex corresponding to $L_mNiX(C_6H_4X)$, complex 1, in high yield,

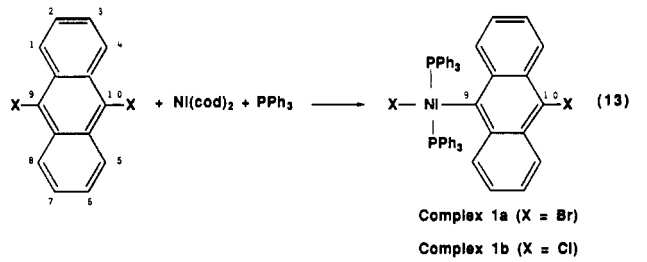


and it has been revealed that the 10-C–X bond in complex 1 is inert against excess Ni(0) complex, presumably due to steric hindrance of the bulky anthryl group and a decrease in electrophilicity of the 10-carbon in complex 1 caused by back donation from nickel. Complex 1 has high thermal and chemical stability; it is stable not only in boiling toluene under air for several hours but also in hydrochloric acid (2 M) in a dispersion system. In the case of complex 1, the steric effect[15a] of the bulky anthryl group as well as partial double bonding between nickel and the aromatic group[17] accounts for the high stability of the Ni–C bond. Due to the extremely high stability of the Ni–C bond, 9,10-$X_2$-Anth does not afford the polymer (run 27). Addition of bpy instead of $PPh_3$ as the neutral ligand does not afford the polymer either. Use of 2,7-$Br_2$-9,10-$H_2$Phen as the monomer (run 28) yields yellow

and fluorescent polymer, $PH_2Phen$, which is partly soluble in $CHCl_3$ and *N*-methylpyrrolidone (NMP).

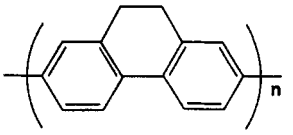

$PH_2Phen$

The yellow color and fluorescent property support that the obtained polymer has a π-conjugation system similar to that of PPP. The IR spectrum of the polymer shows peaks of two categories, one originating from the PPP-like structure (e.g., δ(CH) at 814 $cm^{-1}$) and another from the ethylene unit (e.g., ν(CH) at 2930, 2890, and 2830 $cm^{-1}$). Use of BrCH=CHBr in combination with the mixture of $Ni(cod)_2$ and neutral ligand ($PPh_3$ or bpy) gives a black solid, whose IR spectrum is similar to that of *trans*-poly(acetylene),[18] showing a characteristic sharp absorption peak at 1010 $cm^{-1}$, whereas an attempt to polymerize BrCH=CHBr by the nickel-catalyzed polycondensation with Mg (eq 5) leads to only evolution of gas (presumably acetylene). Since the Ni(0) complex can be generated by electrochemical reduction[19] of the Ni(II) complex and the Ullmann type C–C coupling (eq 4) can be achieved using the electrochemically generated Ni(0) complex,[20] the present polymerization can also be carried out electrochemically starting from the dihaloaromatic compounds as the monomer and Ni(II) complexes (e.g., $[Ni(bpy)_3]Br_2$) as the catalyst. Details of the electrochemical polymerization will be reported elsewhere.

The PPP reported in this paper seem to have a higher molecular weight than the PPP's prepared by the Ni-catalyzed dehalogenation polycondensation of 1,4-$X_2$-Ben (eq 5)[6] and by Kovacic's method,[21] as judged from its IR spectrum and relatively low bromine content. The IR spectrum of the present PPP shows an out-of-plane vibration at 804 ± 2 $cm^{-1}$ (δ(para)) and vibrations of the terminal phenyl unit at 760 (δ($mono_1$)) and 690 $cm^{-1}$ (δ($mono_2$)). It is generally accepted that the *R* value as expressed in eq 14 (where *A* = absorbance) increased with the degree of polymerization of PPP.[6,21]

$$R = \frac{A(\delta(\text{para}))}{A(\delta(\text{mono}_1)) + A(\delta(\text{mono}_2))} \qquad (14)$$

The IR spectrum of the present PPP shows very weak δ($mono_1$) and δ($mono_2$), and the *R* for the present PPP (*R* = 12.7) is much larger than those for PPP's reported by Kovacic and co-workers[21] (*R* = 4.6) and prepared using magnesium as the dehalogenating reagent of 1,4-$Br_2$Ben (eq 5) (*R* = 1.9–3.9). This fact, together with the relatively low content of bromine, indicates that the present PPP has a relatively high degree of polymerization. The present PPP contains 2.7% bromine (cf. Experimental Section). This bromine content corresponds to a molecular weight of 2960 (DP (degree of polymerization) = 38) and 5930 (DP = 76), if the polymer has bromine at one terminal unit and at both terminal units, respectively. If the present PPP has bromine at only one terminal unit, another terminal unit is regarded to be a phenyl group, which is considered to originate from the intermediate Ni($C_6H_4$)–polymer species (cf. eqs 10–12), giving $C_6H_5$–polymer species during workup after polymerization. The CP-MAS $^{13}C$-NMR spectrum of the present PPP (solid) shows peaks at 137 and 127 ppm assigned to the 1,4-carbons and the 2,3-carbons, respectively. No signal assignable to terminal carbon (C–X or C–H) was observable. As for poly(pyridine-2,5-diyl) (Ppy) prepared analogously by using 2,5-dibromopyridine and Ni(0) complex, the polymer is soluble in formic acid and has a degree of polymerization of 20–50 (determined by light scattering) depending on the preparative conditions.[11a,d]

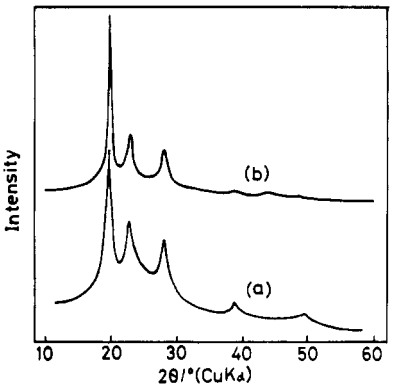


**Figure 1.** Powder X-ray diffraction patterns of PTh (a) and PPP (b).

**Copolymerization.** Copolymerization of 2,5-$Br_2$-Th and 2,4-dibromothiophene (2,4-$Br_2$-Th) as well as that of 2,5-$Br_2$-Th and 1,4-$Br_2$-Ben affords the corresponding copolymers.

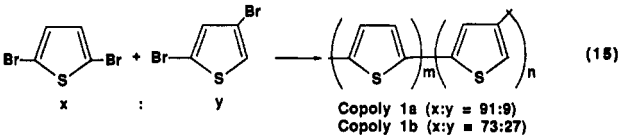


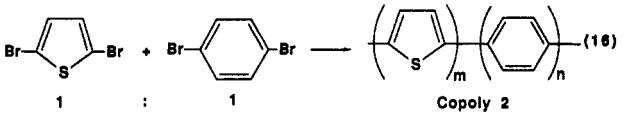


The IR spectrum of copolymer **1** shows δ(CH) absorptions[7c,d] of the thiophene-2,4-diyl unit at 740 and 822 $cm^{-1}$ in addition to the δ(CH) absorption of the thiophene-2,5-diyl unit at 790 $cm^{-1}$. The IR spectrum of copolymer **2** shows the absorption bands from both the thiophene-2,5-diyl and the 1,4-phenylene units. The out-of-plane δ(CH) vibration of copolymer **2** at ~800 $cm^{-1}$ is broadened due to overlapping of the δ(CH) vibrations of the thiophene-2,5-diyl and 1,4-phenylene units.

**Structure and Properties. X-ray and Electron Diffraction of PTh and PPP.** Since the present polymerization is considered to give PTh and PPP with regularly recurring thiophene-2,5-diyl and 1,4-phenylene units, respectively, the polymers are expected to have high crystallinity. The powder X-ray diffraction patterns of the present PTh and PPP give rise to sharp diffraction bands as depicted in Figure 1. PTh and PPP afford the main three X-ray diffraction bands at almost the same 2θ values, and the two polymers are considered to have almost the same two-dimensional structure with the same *ab* parameters[22,23] (the *c*-axis is the direction of the polymer chain). The three main X-ray diffraction bands are regarded to be associated with the diffractions from the *ab* planes.

Vacuum deposition of highly crystalline PTh and PPP on substrates (carbon, gold, aluminum, KBr, etc.) affords thin films of PTh and PPP. The IR spectra of the films deposited on KBr disks are essentially the same as those of the original PTh and PPP. It is reported that PPP with a molecular weight of about 1500–2000, corresponding to a DP of about 20, can be vaporized under vacuum.[24] PTh seems to have a volatileness similar to that of PPP

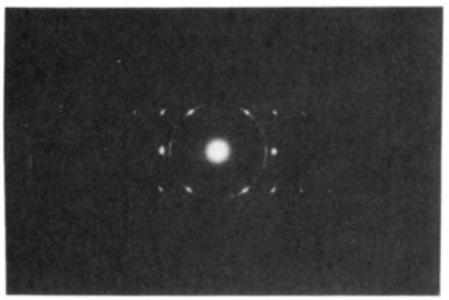

( a )

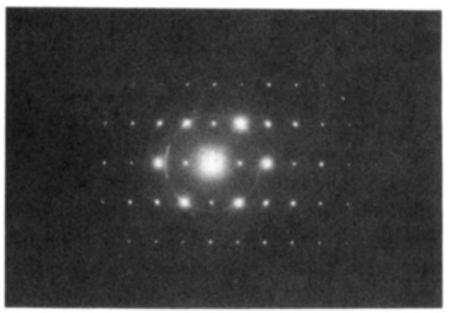

( b )

**Figure 2.** Electron diffraction patterns of PTh (a) and PPP (b) deposited on carbon substrate.

with the same degree of polymerization as judged from the analogous vapor pressure of thiophene and its oligomers ($\alpha$-bithiophene, $\alpha$-terthiophene, etc.) to that of benzene and its oligomers (biphenyl, *p*-terphenyl, etc). Low molecular weight oligomers of PPP and PTh (DP < 17[7d]) are removed from the source materials by Soxhlet extraction with $CHCl_3$. We assume that both the deposited PTh and PPP have a molecular weight of about 1500–2000, corresponding to a DP of 20–25 and to a chain length of 8–10 nm.

Figure 2 shows electron diffraction patterns of the PTh (Figure 2a) and PPP (Figure 2b) films deposited on the carbon substrate at 150 °C. Both the PTh and PPP films have thickness of about 100 nm, corresponding to the stacking of about 10 layers of the PTh and PPP molecules if the molecules are arranged perpendicularly to the surface of the substrate. The electron diffraction patterns are taken with an electron beam (60 keV, corresponding to a wavelength of 5.0 pm) irradiated perpendicularly to the carbon substrate. The observation of regular electron diffraction spots is taken as an indication of the formation of oriented crystalline films of PTh and PPP, and all the spots shown in Figure 2 can be reasonably explained by assuming that PTh and PPP molecules are arranged essentially perpendicularly to the surface of the substrate. Table II summarizes the indexation of the spots shown in Figure 2. As shown in Table II, all of the 14 and 26 observed planar distances calculated from the electron diffraction spots from the PTh and PPP films, respectively, agree within experimental error with the calculated values on the assumed *ab* parameters. Essentially the same *ab* parameters have been reported[22,23,25] mainly based on powder X-ray analysis of PTh and PPP.

Thus, the present results unequivocally indicate that the deposited PTh and PPP molecules take a rodlike rigid linear structure, and the linear molecule is arranged essentially perpendicularly to the surface of the carbon substrate. Similar rodlike linear structure has been confirmed for poly(pyridine-2,5-diyl) with a DP of 20–50

**Table II**
**Planar Distances Estimated from the Electron Diffraction Patterns of PTh and PPP**

| PTh | | | | PPP | | | |
|---|---|---|---|---|---|---|---|
| | planar dist, nm | | | | planar dist, nm | | |
| no. | obsd | calcd[a] | *hkl*[a] | no. | obsd | calcd[a] | *hkl*[a] |
| 1 | 0.78 | 0.78 | 100 | 1 | 0.78 | 0.78 | 100 |
| 2 | 0.56 | 0.56 | 010 | 2 | 0.56 | 0.56 | 010 |
| 3 | 0.45 | 0.45 | 110 | 3 | 0.46 | 0.46 | 110 |
| 4 | 0.40 | 0.39 | 200 | 4 | 0.39 | 0.39 | 200 |
| 5 | 0.32 | 0.32 | 210 | 5 | 0.32 | 0.32 | 210 |
| 6 | 0.28 | 0.28 | 020 | 6 | 0.28 | 0.28 | 020 |
| 7 | 0.26 | 0.26 | 120 | 7 | 0.27 | 0.26 | 300 |
| 8 | 0.26 | 0.26 | 300 | 8 | 0.26 | 0.26 | 120 |
| 9 | 0.24 | 0.24 | 310 | 9 | 0.24 | 0.24 | 120 |
| 10 | 0.23 | 0.23 | 220 | 10 | 0.23 | 0.23 | 220 |
| 11 | 0.20 | 0.20 | 400 | 11 | 0.20 | 0.20 | 400 |
| 12 | 0.19 | 0.20 | 320 | 12 | 0.19 | 0.20 | 320 |
| 13 | 0.19 | 0.18 | 410 | 13 | 0.19 | 0.19 | 030 |
| 14 | 0.16 | 0.16 | 420 | 14 | 0.19 | 0.19 | 410 |
| | | | | 15 | 0.18 | 0.18 | 130 |
| | | | | 16 | 0.17 | 0.17 | 230 |
| | | | | 17 | 0.16 | 0.16 | 420 |
| | | | | 18 | 0.16 | 0.16 | 500 |
| | | | | 19 | 0.16 | 0.15 | 510 |
| | | | | 20 | 0.15 | 0.15 | 330 |
| | | | | 21 | 0.14 | 0.14 | 520 |
| | | | | 22 | 0.14 | 0.14 | 430 |
| | | | | 23 | 0.13 | 0.13 | 600 |
| | | | | 24 | 0.13 | 0.13 | 610 |
| | | | | 25 | 0.12 | 0.12 | 530 |
| | | | | 26 | 0.12 | 0.12 | 620 |

[a] Calculated by assuming an orthorhombic crystal system with $a$ = 0.78 nm and $b$ = 0.56 nm for PTh and $a$ = 0.78 and $b$ = 0.56 nm for PPP.

in a solution as well as in a surface region of poly(vinyl alcohol).[11a,b,d]

In the case of PPP, the perpendicularly oriented crystalline film of PPP is obtained over a relatively wide temperature range of the substrate. However, in the case of PTh, the crystalline and oriented film of PTh is obtained at the substrate temperature of 150 °C, and at lower temperatures the orientation and crystallinity are not so good; at 20 °C only 11 spots and Debye–Scherrer rings are observed. The vacuum deposition of PTh and PPP on gold and aluminum substrates also affords similar thin oriented films which also show electron diffraction patterns similar to those shown in Figure 2. In all cases, the diffraction spots disappear on prolonged irradiation of the electron beam.

It is interesting that not only the first molecular layer of PTh or PPP directly contacting the surface but also the PTh or PPP molecules in the upper layers are oriented perpendicularly to the surface of the substrate. Since PTh and PPP have almost the same crystal parameters for the *ab* plane (Table II), the matching of PTh and PPP along the direction of the polymer chain will be good, and it may be possible to obtain a mixed oriented layer of PTh and PPP where layers of PTh and PPP are stacked alternately (a kind of superlattice).

In contrast to the orientation of PTh and PPP perpendicularly to the surface of the substrate, vacuum deposition of PTh on a rubbed polyimide film, which is now widely used for orientation of liquid crystals along the direction of rubbing, leads to another type of orientation of PTh.

Irradiation of polarized UV–visible light to the polyimide film containing the vacuum-deposited PTh in its surface region showed the $\pi$–$\pi^*$ absorption peak at 430 nm and reveals dichroism[11d] for the absorption peak. The

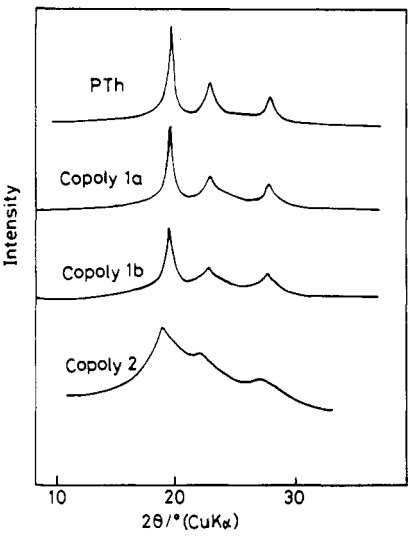


**Figure 3.** Powder X-ray diffraction patterns of PTh and its copolymers.

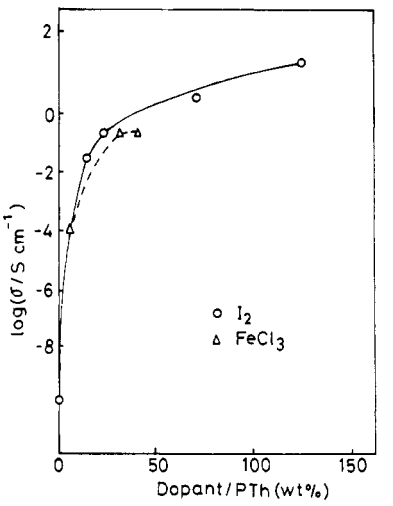


**Figure 4.** Dependence of electrical conductivity ($\sigma$) of the doped PTh on the amount of dopant. Measured with pellet formed by pressing the doped powdery sample. $T \sim 25$ °C.

absorbance of the $\pi$–$\pi^*$ absorption peak varied with the angle ($\theta$) between the direction of the oscillating electric field of the polarized light and the direction of rubbing of the polyimide. The absorbance of the peak at $\theta = 0°$ ($a_\parallel$) was larger than the absorbance ($a_\perp$) observed at $\theta = 90°$ ($a_\parallel/a_\perp = 1.5$), indicating that the polymer chain of PTh was oriented to some extent along the direction of the rubbing.

**Structure of Other Polymers.** The powder X-ray diffraction pattern of the present PRTh shows only broad diffraction bands, revealing that most of the polymer is amorphous. The degree of depolarization ($\rho_v$) of a chloroform solution of PRTh (R = $n$-$C_6H_{13}$) measured by irradiation of a polarized Ar laser is 0, indicating that PRTh adopts a random-coil structure in the solution. Steric repulsion between the R groups may prevent PRTh from adopting a linear structure such as those of PTh and PPP in the solid state. The specific refractive index increment $\Delta n/\Delta c$ of PRTh in DMF measured by Ar laser irradiation (488 nm), $\Delta n/\Delta c = 0.35$ cm$^3$ g$^{-1}$, is considerably higher than those of usual non-$\pi$-conjugated polymers ($\Delta n/\Delta c$ = 0.1–0.2 cm$^3$ g$^{-1}$).

This reveals that PRTh has a large refractive index, presumably reflecting the presence of mobile electrons along the $\pi$-conjugation system. Poly(9,10-dihydrophenanthrene-2,7-diyl) ($PH_2Phen$) obtained by the polymerization of 2,7-$Br_2$-9,10-$H_2$Phen gives rise to somewhat broad diffraction bands with $d$-spacings of 0.49, 0.39, 0.35, and 0.21 nm in its powder X-ray diffraction pattern. The X-ray diffraction patterns is considerably different from that of PPP as anticipated from the presence of the $-CH_2CH_2-$ unit in addition to the PPP main framework.

Copolymer **1b** and copolymer **2** have lower crystalline order than PTh and PPP as judged from broader diffraction bands observed in their powder X-ray diffraction patterns (Figure 3), although the powder X-ray diffraction pattern of copolymer **1a** with a low content of thiophene-2,4-diyl unit shows diffraction peaks with almost the same sharpness as that of the diffraction peaks of PTh. In the case of copolymer **2**, the difference in the spacing along the polymer chain between the thiophene-2,5-diyl unit and the 1,4-phenylene unit seems to prevent the copolymer from forming good microcrystals, in spite of matching of the two-dimensional crystal structure with almost the same $ab$ parameters (vide ante). According to the previously reported powder X-ray diffraction analysis,[22,23] the thiophene-2,5-diyl and 1,4-phenylene units seem to have 400- and 420-pm spacing, respectively.

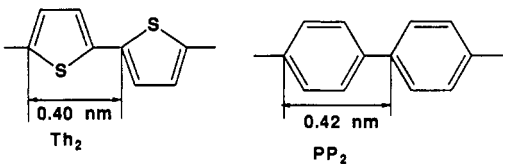


**Doping and Electrically Conducting Properties.** Doping of the present PTh with iodine and $FeCl_3$ affords electrically conducting material, and the dependence of the electrical conductivity ($\sigma$) on the amount of iodine and $FeCl_3$ added is depicted in Figure 4. The $\sigma$ values of the iodine and $FeCl_3$ adducts of the present PTh are comparable to or higher than those of similar adducts of PTh previously prepared by the Ni-catalyzed dehalogenation condensation (eq 5 etc.).[7,26]

Figures 5 and 6 show the change of the IR spectra and powder X-ray diffraction patterns, respectively, of the present PTh on the doping with iodine and undoping with hydrazine. The doping causes a profound change in the IR spectrum even at a relatively low doping level (iodine/PTh = 16–40 wt %, spectra b and c in Figure 5) presumably due to the change in the electronic state of PTh. The iodine doping causes broadening of the X-ray diffraction peaks at the relatively low doping level; however, at 16 wt % of iodine per PTh (pattern b in Figure 6) no new peak is observable.

At 40 wt % of iodine per PTh (pattern c in Figure 6), a small broad rise at about $2\theta = 9°$ (Cu K$\alpha$) appears in addition to the broadening of the diffraction peaks. At 69 wt % of iodine (pattern d), the peak at about $2\theta = 9°$ due to partial formation of a new structure becomes distinct, and when PTh is extensively doped (saturation doping) with iodine (120 wt %, pattern e), the X-ray diffraction pattern is entirely changed, demonstrating formation of a new structure. Similar formation of new structures by incorporation of dopants has been reported for p-type doping of poly(acetylene)[27] and PPP[28] prepared by another method.

The four X-ray diffraction peaks observed for the extensively iodine-doped PTh at $2\theta = 8.8$, 18.0, 27.0, and 36.1° correspond to $d$ values of 1.00, 0.49, 0.33, and 0.25 nm. The appearance of the X-ray diffraction peaks at $d = a/n$ ($a = 1.00$ nm, $n = 1, 2, 3, 4$) indicates one-dimensional crystalline order with a period of 1.00 nm.

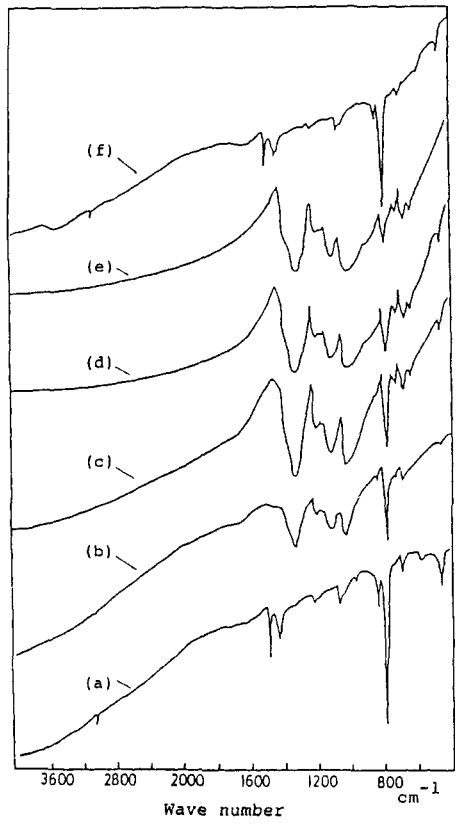


**Figure 5.** Change of IR spectrum of PTh on doping with iodine and undoping with hydrazine: (a) original PTh; (b) iodine/PTh (wt/wt) = 0.16; (c) iodine/PTh = 0.40; (d) iodine/PTh = 0.69; (e) iodine/PTh = 1.20 (saturation doping); (f) undoped with hydrazine.

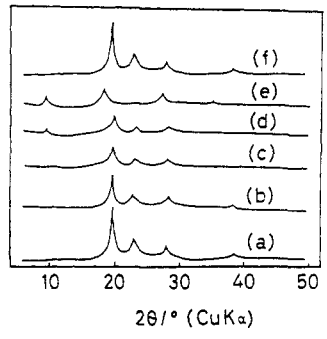


**Figure 6.** Change of powder X-ray diffraction pattern of PTh on doping with iodine and undoping with hydrazine. a–f as in Figure 5.

On the basis of points a–e which follow, saturately doped PTh seems to have the structure as illustrated in Figure 7.

(a) In the iodine-doped PTh, iodine seems to exist as a polyiodide anion $I_5^-$, [I–I–I···I–I]$^-$, which is considered to have a length of ~1.7 nm, as revealed by resonance Raman and $^{129}I$ Mössbauer spectroscopy.[29]

(b) As described above, two thiophene-2,5-diyl units ($Th_2$) in PTh take a repeat distance of ~0.80 nm, and doping with iodine presumably causes elongation of the distance due to a partial shift of electrons from PTh to iodine.

(c) The diameter of an iodine atom is ~0.4 nm, and the PTh plane seems to have a van der Waals dimension of about 0.65 × 0.36 nm[22b,30] when the PTh molecule is viewed from the direction of the *c*-axis.

(d) The saturately iodine-doped PTh showing the distinct four new diffraction peaks (pattern e in Figure 6) contains 120 wt % of iodine per PTh.

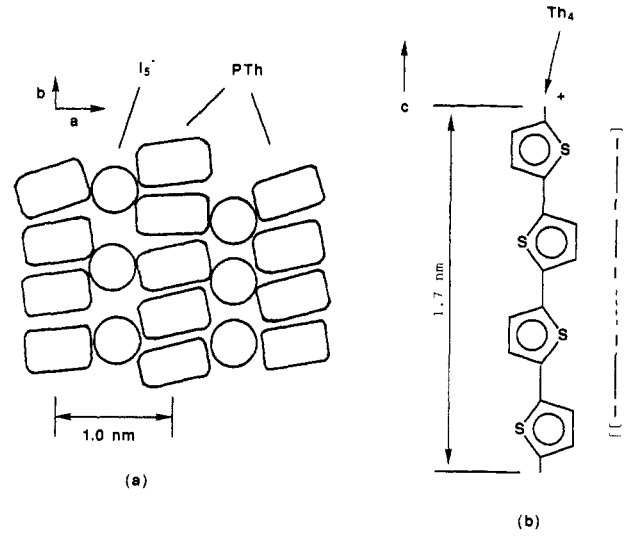


**Figure 7.** Proposed structure of PTh saturately doped with iodine.

(e) In the two-dimensional rectangular unit cell of undoped PTh with $a = 0.78$ nm and $b = 0.56$ nm, PTh planes are stacked in the *b*-axis direction as analyzed by Bruckner and Porzio[22b] based on the powder X-ray diffraction pattern, and doping with iodine may expand the *a*-axis.

In Figure 7, the length of the four thiophene-2,5-diyl units ($Th_4$) roughly fits the length (1.7 nm) of [I–I–I···I–I]$^-$, and the 120 wt % of iodine per PTh corresponds to about a 5:8 molar ratio between [I–I–I···I–I]$^-$ and $Th_4$. The observed strength ratios between the four new X-ray diffraction peaks of the saturately doped PTh (Figure 6e) roughly agree with calculated values based on this 5:8 molar ratio.

The IR spectrum and powder X-ray diffraction pattern (curves f in Figures 5 and 6) after the undoping of the iodine-doped PTh with hydrazine are essentially the same as those of the original PTh. Elemental analysis also indicates the occurrence of complete undoping. These results clearly indicate that the reversibility of the doping and undoping processes of PTh using iodine and hydrazine is very good, in view of not only the chemical structure but also the crystal structure of the polymer. The electrical conductivity of the iodine-doped PTh remained almost constant for at least 4 months.

Doping of PTh with $FeCl_3$ led to the appearance of new broad diffraction peaks at about $2\theta = 15.5$, 19.5, and 26.5° (Cu K$\alpha$). When the extensively $FeCl_3$-doped PTh was treated with the aqueous solution of hydrazine, the reddish color of PTh was recovered and the IR spectrum of the hydrazine-treated sample was essentially the same as that of the original PTh. However, the powder X-ray diffraction peaks of the hydrazine-treated sample were much broader than those of the original PTh, indicating that recovery of the original crystal form after loss of the $FeCl_3$-originated dopant (presumably $FeCl_4^-$)[26] was not sufficient. Thus, in the case of the $FeCl_3$ doping, the reversibility of the doping and undoping processes was not good; the occurrence of chemical reaction in PTh caused by $FeCl_3$ or the difficulty in rearrangement of the PTh molecule after removal of the dopant explains the result. It is known that $FeCl_3$ leads to coupling between aromatic rings by oxidation of aromatic compounds such as pyrrole and thiophene.[13]

Doping of the present PTh with sodium gives a black semiconducting material with an electrical conductivity ($\sigma$) of $2 \times 10^{-7}$ S cm$^{-1}$. Figure 8 shows cyclic voltammograms of PRTh (R = *n*-$C_6H_{13}$) film on a platinum electrode.

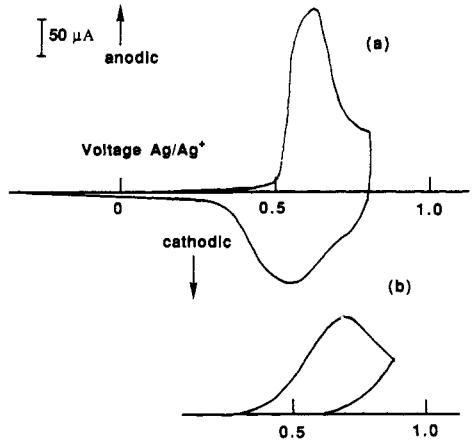


**Figure 8.** Cyclic voltammograms of PRTh (R = $n$-$C_6H_{13}$) on a Pt electrode. (a) in a $CH_3CN$ solution of $[N(C_4H_9)_4]BF_4$ (0.10 M); (b) in a solution of $[N(n\text{-}C_4H_9)_4][SO_3\text{-}p\text{-}C_6H_4CH_3]$ (0.10 M). Sweep rate = 10 mV $s^{-1}$.

The oxidation–reduction or doping–undoping potentials are almost the same as those[31] reported for PRTh prepared by other methods. In most cases, the potential giving the peak anodic current, $E_{p_a}$, is virtually independent on the kind of anion in $[N(n\text{-}C_4H_9)_4]Y$ (for $Y = ClO_4^-$, $BF_4^-$, and $PF_6^-$, $E_{p_a}$ = 0.58–0.61 V vs $Ag/Ag^+$), and the normal cyclic voltammogram is obtained with a doping level of about 0.19 as estimated from the anodic current. However, when doping is carried out with a relatively large anion, for example by using $[N(n\text{-}C_4H_9)_4][SO_3\text{-}p\text{-}C_6H_4CH_3]$, the $E_{p_a}$ position shifts to a higher oxidation potential ($E_{p_a}$ = 0.78 vs $Ag/Ag^+$) and undoping current is not observable (Figure 8b), suggesting that doping with a large anion is a rather difficult process and that once the polymer is doped with the anion, undoping is very difficult. The change of the UV–visible spectrum of PRTh on an ITO electrode on the doping and undoping processes is almost the same as that reported for PRTh prepared by other methods.[31]

Exposure of poly(3-cyanothiophene-2,5-diyl) to a vapor of iodine affords an adduct with iodine; however, the electrical conductivity is low ($\sigma = 10^{-9}$ S $cm^{-1}$), presumably due to the difficulty of forming a positive carrier by electron transfer from the polymer with the electron-withdrawing CN group to iodine. Sodium doping of poly(3-cyanothiophene-2,5-diyl) affords a semiconducting material with a $\sigma$ value of $10^{-6}$ S $cm^{-1}$. Doping of the present PPP with sodium and iodine yields semiconducting adducts, both of which show a $\sigma$-value of $\sim 7 \times 10^{-5}$ S $cm^{-1}$.

The cyclic voltammogram of $PH_2Phen$ on a Pt electrode gives rise to a doping peak potential and undoping peak potential at 1.04 and 0.78 vs $Ag/Ag^+$, respectively, in a $CH_3CN$ solution of $[N(C_2H_5)_4]ClO_4$. These potentials agree with the corresponding potentials[32] of PPP prepared by previously reported methods, indicating that $PH_2Phen$ has essentially the same $\pi$-conjugation system as that of PPP. The 1:1 copolymer of 2,5-dibromothiophene and 1,4-dibromobenzene also yields a semiconducting material with a $\sigma$-value of $9 \times 10^{-6}$ S $cm^{-1}$ on doping with iodine, whereas a sodium-doped copolymer is an insulator.

## Conclusions

Dehalogenation polycondensation of 2,5-dihalothiophene and 1,4-dihalobenzene affords PTh and PPP, respectively, with linear structure and high crystallinity in high yields. Vacuum deposition of PTh and PPP gives crystalline films of the polymers with their main chain essentially perpendicular to the surface of substrates such as carbon and gold. Doping of PTh with iodine and $FeCl_3$ gives semiconducting adducts, and the doping–undoping process of PTh with iodine and hydrazine is reversible from the viewpoint of not only chemical structure but also packing structure in the solid state. PRTh is electrochemically active in the p-doping region. $PH_2Phen$ has essentially the same $\pi$-conjugation system as that of PPP although the crystallinity of $PH_2Phen$ is low.

## Experimental Section

**Materials.** Commercially available 2,5-dihalothiophene (purity >99%), 1,4-dihalobenzene, 4,4′-dibromobiphenyl, 9,10-dihaloanthracene, and BrCH=CHBr were used as purchased. 2,5-Diiodo-3-alkylthiophenes[8c,33] and 2,5-dibromo-3-cyanothiophene[34] were prepared according to the literature. 2,7-Dibromo-2,10-dihydrophenanthrene was kindly donated by General Oil Co. Ltd. $Ni(cod)_2$[35a] and $Ni(PPh_3)_4$[35b] were prepared as reported in the literature. 2,2′-Bipyridyl (bpy) and triphenylphosphine ($PPh_3$) were used as purchased. Solvents were dried, distilled, and stored under argon or $N_2$. Supporting salts like $[N(C_2H_5)_4]Y$ (Y = $ClO_4$, $BF_4$, etc.) were recrystallized and dried before use.

**Polymerization.** $Ni(cod)_2$ (1.59 g, 6.00 mmol), 1,5-cyclooctadiene (531 mg, 5.00 mmol), and bpy (937 mg, 6.00 mmol) were dissolved in 20 mL of DMF in a Schlenk tube under argon. To the solution was added 2,5-dibromothiophene (1.21 g, 5.00 mmol) at room temperature. The reaction mixture was stirred at 60 °C for 16 h to yield a reddish brown precipitate. The reaction mixture was then poured into HCl–acidic methanol, and the precipitate of PTh was separated by filtration. The filtrate was washed with HCl–acidic methanol, ethanol, hot toluene, a hot aqueous solution of ethylenediaminetetraacetic acid (EDTA, pH = 3.80), a hot aqueous solution of EDTA (pH = 9), and distilled water in this order and dried under vacuum to yield a reddish brown powder of PTh. Anal. Found (no. 3 in Table I): C, 58.2; H, 2.4; S, 36.0; Br, 0.7. Calcd for $(C_4H_2S)_n$: C, 58.5; H, 2.5; S, 39.0. A part of the difference between the found and calculated values seems to be attributable to the high thermal stability of the polymer. Other polymerizations listed in Table I were carried out analogously. 1 (R = $n$-$C_6H_{13}$): Anal. Found: C, 72.1; H, 8.4; S, 18.4. Calcd for $(C_{10}H_{18}S)_n$: C, 72.3; H, 8.4; S, 19.3. 1 (R = $n$-$C_8H_{10}$): Anal. Found: C, 73.7; H, 9.8; S, 16.6; I, 1.9. Calcd for $(C_{12}H_{20}S)$: C, 74.2; H, 9.3; S, 16.5. PPP: Anal. Found: C, 93.1; H, 5.7; Br, 2.7. Calcd for $(C_6H_4)_n$: C, 94.7; H, 5.3. $PH_2Phen$: Anal. Found: C, 91.5; H, 5.7; Br, 1.3. Calcd for $(C_{14}H_{10})_n$: C, 94.3; H, 5.7.

**Preparation of Anthrylnickel Complex 1.** A THF (15 mL) solution of 9,10-dibromoanthracene (1.0 g, 2.9 mmol) was added to a THF (18 mL) solution containing $Ni(cod)_2$ (0.90 g, 3.3 mmol), cod (0.7 mL), and $PPh_3$ (1.73 g, 6.6 mmol) at room temperature. Stirring the reaction mixture for 8 h at 60 °C afforded a yellow precipitate, which was separated by filtration, washed with toluene, recrystallized from THF, and dried under vacuum to yield 2.42 g (90%) of complex **1a**. Anal. Found: C, 65.0; H, 4.1; Br, 17.7. Calcd: C, 65.3; H, 4.1; Br, 17.4. Mp 217 °C (dec). A similar procedure using 9,10-dichloroanthracene affords complex **1b**. Anal. Found: C, 72.0; H, 4.8; Cl, 8.1. Calcd: C, 72.3; H, 4.6; Cl, 8.5.

**Measurement.** IR spectra were recorded on a JASCO IR-810 spectrometer. NMR spectra in solutions and solid-state NMR spectra were taken using JEOL JNM-GX-500 and JEOL JNM-GX-270 spectrometers, respectively. X-ray diffraction patterns were recorded on a Philips PS-1051 instrument. Electron diffraction patterns were taken by Mr. R. Ohki of our institute with a JEOL JEM-100-CX diffractometer. KBr pellet substrate was prepared by pressing KBr powder at 600 kg $cm^{-1}$. Carbon (amorphous) substrate was prepared on a collodion film by vacuum deposition or sputtering. Gold and aluminum were deposited on the carbon substrate to afford the gold and aluminum substrates, respectively. Rubbed polyimide (No. AL-1051 produced by Japan Synthetic Rubber Co. Ltd.) film substrate on a glass plate was kindly donated by Nippon Electric Co. Ltd.

GPC curves, TGA curves, and UV–visible spectra were measured with a Shimadzu liquid chromatography system with a Shodex 80M column and a 6A refractive index detector (solvent = $CHCl_3$), a Shimadzu thermoanalyzer DT-30, and a Hitachi

Model 200-20 spectrometer, respectively. Molecualr weight measurement of PRTh by light scattering as well as measurement of the degree of depolarization ($\rho_v$) and the refractive index increment ($\Delta n/\Delta c$) was carried out as previously reported.[36]

Cyclic voltammetry was carried out with a Hokuto Denko HA-501 galvanostat/potentiostat and a Hokuto Denko KB-104 function generator. PRTh (R = $n$-$C_6H_{13}$, $3.8 \times 10^{-5}$ g, $2.4 \times 10^{-7}$ mol of monomer unit) was laid on the Pt electrode ($1.0 \times 1.0$ cm) by painting the electrode with a $CHCl_3$ solution of PRTh and then evaporating the $CHCl_3$; with this electrode the cyclic voltammogram was measured. The electrical conductivity was measured with a Takeda Riken TR-8651 electrometer. Elemental analysis was carried out by Mrs. M. Tanaka of our laboratory with a Yanagimoto CHN Autocorder Type MT-2 (analysis of C, H, N) and at Kyoto University (analysis of S and halogen).

**Doping and Undoping.** PTh was exposed to a vapor of iodine in a vacuum line or to a $CH_3NO_2$ solution of $FeCl_3$ under argon. For the iodine-doped PTh, the excess iodine was removed under vacuum for 10 h at room temperature, and the amount of iodine taken into the polymer was measured. The $FeCl_3$-doped PTh was washed with $CH_3NO_2$ and dried under vacuum. The amount of $FeCl_3$ taken was calculated from analytical data of the adduct.

A THF solution of sodium naphthalide was prepared with sodium (200 mg, 8.7 mmol) and naphthalene (400 mg, 3.1 mmol) in 20 mL of THF. To this THF solution was added the powdery PTh (100 mg), and the reaction mixture was stirred for 24 h at room temperature under argon to yield a black precipitate. After separation of the black precipitate by filtration under argon, it was dried under vacuum.

Each of the powdery doped PTh samples was pressed at 200 kg $cm^{-1}$ to obtain a pellet, from which a bar (e.g., 1 mm × 3 mm × 13 mm) was cut off. After putting electrodes at the ends of the bar with Electrodag (carbon-polymer paste from Furuuchi Chemical Co. Ltd.), the electrical conductivity was measured. Chemical doping and measurement of the electrical conductivity of other polymer were carried out analogously. The Pt electrode (1 cm × 1 cm) was painted with a $CHCl_3$ solution of PRTh or an NMP solution of $PH_2Phen$. After removal of solvent by natural evaporation or vacuum evaporation, the electrode was dipped in an electrolytic solution and the cyclic voltammograms were taken.

**Vacuum Deposition.** PTh and PPP were evaporated from a tantalum boat heated to 250–300 °C at $10^{-4}$ Pa by using an EBV-6DA type vacuum evaporation apparatus produced by ULVAC Co. Ltd. The thicknesses of the deposited PTh and PPP films were determined by the multiple-beam interfering method with a Type 2 reflection interferometer produced by Kojiri Optics Co. Ltd.

## References and Notes


(1) Yamamoto, T.; Yamamoto, A.; Ikeda, S. *J. Am. Chem. Soc.* **1971**, *93*, 3350, 3360; Kohara, T.; Yamamoto, T.; Yamamoto, A. *J. Organomet. Chem.* **1980**, *192*, 265; Tatsumi, K.; Nakamura, A.; Komiya, S.; Yamamoto, T.; Yamamoto, A. *J. Am. Chem. Soc.* **1984**, *106*, 8181; Komiya, S.; Abe, Y.; Yamamoto, A.; Yamamoto, T. *Organometallics* **1983**, *2*, 1466.

(2) (a) Jolly, P. W.; Wilke, G. *The Organic Chemistry of Nickel*; Academic Press: New York, 1974; Vol. I, p 206; (b) Collman, J. P.; Hegedus, L. S.; Norton, J. R.; Finke, R. G. *Principles and Applications of Organotransition Metal Chemistry*; University Science Books: Mill Valley, CA, 1987; p 322; (c) Kochi, J. K. *Organometallic Mechanisms and Catalysis*; Academic Press: New York, 1978; (d) Tamao, K.; Kumada, M. In *The Chemistry of the Metal-Carbon Bond*; Hartley, F. R., Ed.; Interscience: New York, 1987; Vol. 4, p 819; (e) Yamamoto, A. *Organotransition Metal Chemistry*; John Wiley: New York, 1986; p 244; (f) Pearson, A. J. *Metalloorganic Chemistry*; John Wiley: New York, 1985; p 36; (g) Akermark, B.; Ljungqvist, A. *J. Organomet. Chem.* **1978**, *149*, 97; (h) Akermark, B.; Johansen, H.; Roos, B.; Wahlgren, U. *J. Am. Chem. Soc.* **1979**, *101*, 5876; (i) Binger, P.; Doyle, M. J. *J. Organomet. Chem.* **1978**, *162*, 195.

(3) Tamao, K.; Sumitani, K.; Kiso, Y.; Zembayashi, M.; Fujioka, A.; Kodama, K.; Nakajima, I.; Minato, A.; Kumada, M. *Bull. Chem. Soc. Jpn.* **1976**, *49*, 1958; Morrell, D. G.; Kochi, J. K. *J. Am. Chem. Soc.* **1975**, *97*, 7262.

(4) Kende, A. S.; Liebeskind, L. S.; Braitsch, D. M. *Tetrahedron Lett.* **1977**, 3375; Iyoda, M.; Sakitani, M.; Otsuka, H.; Oda, M. *Chem. Lett.* **1985**, 127; Zembayashi, M.; Tamao, K.; Yoshida, J.; Kumada, M. *Tetrahedron Lett.* **1977**, 4089.

(5) Semmelhack, M. F.; Helquist, P. M.; Jones, L. D. *J. Am. Chem. Soc.* **1971**, *93*, 5903; Semmelhack, M. F.; Ryono, L. S. *J. Am. Chem. Soc.* **1975**, *97*, 3873; Kende, A. S.; Kiebeskind, L. S.; Braitsch, D. M. *Tetrahedron Lett.* **1975**, 3375; Tiecco, M.; Testaferri, L.; Tingoli, M.; Chianelli, D.; Montucci, M. *Synthesis* **1984**, 736; Jolly, P. W.; Wilke, G. *The Organic Chemistry of Nickel*; Academic Press: New York, 1975; Vol. II, p 246.

(6) Yamamoto, T.; Hayashi, Y.; Yamamoto, A. *Bull. Chem. Soc. Jpn.* **1978**, *51*, 2091; Czerwinski, W. *Synth. Met.* **1990**, *35*, 229; Brown, C. E.; Kovacic, P.; Wilkie, C. A.; Kinsinger, J. A.; Hein, R. E.; Yaniger, S. I.; Cody, R. B., Jr. *J. Polym. Sci., Polym. Chem. Ed.* **1986**, *24*, 255.

(7) (a) Sanechika, K.; Yamamoto, T.; Yamamoto, A. *Polym. Prepr. Jpn.* **1979**, *28*, 966; (b) Yamamoto, T.; Sanechika, K.; Yamamoto, A. *J. Polym. Sci., Polym. Lett. Ed.* **1980**, *18*, 9; (c) Sanechika, K.; Yamamoto, T.; Yamamoto, A. *Ibid.* **1982**, *20*, 365; (d) Yamamoto, T.; Sanechika, K.; Yamamoto, A. *Bull. Chem. Soc. Jpn.* **1983**, *56*, 1497, 1503; (e) Colon, I.; Kwiatkowski, G. T. *J. Polym. Sci., Polym. Chem. Ed.* **1990**, *28*, 367; (f) Yamamoto, T.; Osakada, K.; Wakabayashi, T.; Yamamoto, A. *Makromol. Chem., Rapid Commun.* **1985**, *6*, 671; (g) Kobayashi, M.; Chen, J.; Moraes, T.-C.; Heeger, A. J.; Wudl, F. *Synth. Met.* **1984**, *9*, 77; (h) Hotz, C.; Kovacic, P.; Khoury, I. A. *J. Polym. Sci., Polym. Chem. Ed.* **1983**, *21*, 2617; (i) Cao, Y.; Wu, Q.; Guo, K.; Qian, R. *Makromol. Chem.* **1984**, *185*, 389; (j) Brown, C. E.; Kovacic, P.; Cody, R. B., Jr.; Hein, R. E.; Kinsinger, J. A. *J. Polym. Sci., Polym. Lett. Ed.* **1986**, *24*, 519.

(8) (a) Yamamoto, T.; Sanechika, K. *Chem. Ind. (London)* **1982**, 301; (b) Yamamoto, T.; Sanechika, K.; Yamamoto, A. U.S. Patent 1985, 4,521,589; (c) Elsenbaumer, R. S.; Jen, K. Y.; Oboodi, R. *Synth. Met.* **1986**, *15*, 169; (d) Czerwinski, A.; Cunningham, D. D.; Amer, A.; Schrader, J. R.; Pham, C. V.; Zimmer, H.; Mark, H. B., Jr. *J. Electrochem. Soc.* **1987**, *134*, 1158; (e) Österholm, J.-E.; Laakso, J.; Nyholm, P.; Isotalo, H.; Stubb, H.; Inganäs, O.; Salaneck, W. R. *Synth. Met.* **1989**, *28*, C435.

(9) Khoury, I.; Kovacic, P.; Gilow, H. M. *J. Polym. Sci., Polym. Lett. Ed.* **1981**, *19*, 395.

(10) Sanechika, K.; Yamamoto, T.; Yamamoto, A. *Polym. J.* **1981**, *13*, 255; Yamamoto, T.; Sanechika, K.; Yamamoto, A.; Katada, M.; Motoyama, I.; Sano, H. *Inorg. Chim. Acta* **1983**, *73f*, 75.

(11) (a) Yamamoto, T.; Ito, T.; Kubota, K. *Chem. Lett.* **1988**, 153; (b) Yamamoto, T.; Maruyama, T.; Ikeda, T.; Sisido, M. *J. Chem. Soc., Chem. Commun.* **1990**, 1306; (c) Zotti, G.; Schiavon, G. *J. Electroanal. Chem.* **1984**, *163*, 385; (d) Yamamoto, T.; Maruyama, T.; Kubota, K. *Chem. Lett.* **1989**, 1951.

(12) Swager, T. M.; Grubbs, R. H. *J. Am. Chem. Soc.* **1989**, *111*, 4413; Ryoo, M.-S.; Lee, W.-C.; Choi, S.-K. *Macromolecules* **1990**, *23*, 3029; Cho, O.-K.; Kim, Y.-H.; Choi, K.-Y.; Choi, S.-K. *Ibid.* **1990**, *23*, 12.

(13) Hotta, S.; Soga, M.; Sonoda, N. *Synth. Met.* **1988**, *26*, 267; Yoshino, K.; Hayashi, S.; Sugimoto, R. *Jpn. J. Appl. Phys.* **1984**, *23*, L899; Sugimoto, R.; Takeda, S.; Yoshino, K. *Chem. Express* **1986**, *1*, 635.

(14) (a) Roncali, J.; Garreau, R.; Yassar, A.; Marque, P.; Garnier, F.; Lemaire, M. *J. Phys. Chem.* **1987**, *91*, 6706; (b) Sato, M.; Tanaka, S. Kaeriyama, K. *Synth. Met.* **1986**, *14*, 275; (c) Sato, M.; Tanaka, S.; Kaeriyama, K. *Makromol. Chem.* **1987**, *188*, 1763; (d) Bryce, M. R.; Chissel, A.; Kathirgamanathan, P.; Paker, D.; Smith, N. R. M. *J. Am. Chem. Soc., Chem. Commun.* **1987**, 466; (e) Maior, R. M. S.; Hinkelmann, K.; Eckert, H.; Wudl, F. *Macromolecules* **1990**, *23*, 1268.

(15) (a) Hidai, M.; Kashiwagi, T.; Ikeuchi, T.; Uchida, Y. *J. Organomet. Chem.* **1971**, *30*, 279; (b) Yamamoto, T.; Kohara, T.; Yamamoto, A. *Bull. Chem. Soc. Jpn.* **1981**, *54*, 1720, 2010, 2161.

(16) (a) Parhall, G. W. *J. Am. Chem. Soc.* **1974**, *96*, 2360; (b) Morrell, D. G.; Kochi, J. K. *Ibid.* **1975**, *97*, 7262; (c) Komiya, S.; Albright, T.; Hoffmann, R.; Kochi, J. K. *Ibid.* **1976**, *98*, 7255; **1977**, *99*, 8840; (d) Ozawa, F.; Kurihara, K.; Yamamoto, T.; Yamamoto, A. *Bull. Chem. Soc. Jpn.* **1985**, *58*, 399.

(17) Chatt, J.; Shaw, B. L. *J. Chem. Soc.* **1960**, 1719. Preliminary X-ray structural analysis of complex **1a** revealed a shorter Ni–C bond length (187 pm) than the usual Ni–C bond length (Churchill, M. R.; Kalra, K. L.; Veidis, M. V. *Inorg. Chem.* **1983**, *12*, 1656 and ref 2a), supporting the partial formation of double bonding. The large p-system of the anthryl group may facilitate Ni–C double bonding.

(18) Shirakawa, H.; Ikeda, S. *Polym. J.* **1971**, *2*, 231.

(19) Bontempelli, G.; Magno, F.; Corain, B.; Schiavon, G. *J. Electroanal. Chem.* **1979**, *103*, 243; Bontempelli, G.; Magno, F.; Daniele, S.; Schiavon, G. *Ibid.* **1983**, *159*, 117.

(20) Mori, M.; Hashimoto, Y.; Ban, Y. *Tetrahedron Lett.* **1980**, *21*, 631.

(21) Kovacic, P.; Oziomek, J. *J. Org. Chem.* **1964**, *29*, 101.

(22) (a) Mo, Z.; Lee, K.-B.; Moon, Y. B.; Kobayashi, M.; Heeger, A. J.; Wudl, F. *Macromolecules* **1985**, *18*, 1972; (b) Bruckner, S.; Porzio, W. *Makromol. Chem.* **1988**, *189*, 961.
(23) (a) Kovacic, P.; Feldman, M. B.; Kovacic, J. P.; Lando, J. B. *J. Appl. Polym. Sci.* **1968**, *12*, 1735; (b) Froyer, G.; Maurice, F.; Mersicer, J. P.; Riviere, D.; Le Cun, M.; Auvray, P. *Polymer* **1981**, *22*, 992; (c) Schacklette, L. W.; Chance, R. R.; Ivory, D. M.; Miller, G. G.; Baughmann, R. H. *Synth. Met.* **1979**, *1*, 307; (d) Sasaki, S.; Yamamoto, T.; Kanbara, T.; Morita, A.; Yamamoto, T., submitted to *J. Polym. Sci.*
(24) Brown, C. E.; Kovacic, P.; Wolkie, C. A.; Cody, R. B., Jr.; Kinsinger, J. A. *J. Polym. Sci., Polym. Lett. Ed.* **1985**, *23*, 453 and mass spectra in this reference.
(25) Yamamoto, T.; Kanbara, T.; Mori, C. *Synth. Met.* **1990**, *38*, 399.
(26) Yamamoto, T.; Sanechika, K.; Sakai, H. *J. Macromol. Sci., Chem.* **1990**, *A27*, 1147.
(27) Perogo, G.; Laugli, G.; Pedretti, U.; Allegra, G. *Makromol. Chem.* **1988**, *189*, 2687; Baughmann, R. H.; Murthy, N. S.; Miller, G. G.; Shacklette, L. W. *J. Chem. Phys.* **1983**, *79*, 1066; Chien, J. C. W.; Karasz, F. E.; Shimamura, K. *Macromolecules* **1982**, *15*, 1012.
(28) Rueda, D. R.; Cagiao, M. E.; Belta Calleja, F. J. *Polym. Bull.* **1989**, *21*, 635; Hasslin, H. W.; Riekel, C. *Synth. Met.* **1982**, *5*, 37.
(29) Sakai, H.; Mizota, M.; Maeda, Y.; Yamamoto, T.; Yamamoto, A. *Bull. Chem. Soc. Jpn.* **1985**, *58*, 926.
(30) Bondi, A. *J. Phys. Chem.* **1964**, *68*, 441.
(31) Roncali, J.; Marque, P.; Garrequ, R.; Garnier, F.; Lemaire, M. *Macromolecules* **1990**, *23*, 1347.
(32) Schiavon, G.; Zotti, G.; Bontempelli, G. *J. Electroanal. Chem.* **1984**, *161*, 323.
(33) Baker, J.; Huddleston, P. R.; Wood, M. L. *Synth. Commun.* **1975**, *5*, 59.
(34) Fournari, P.; Gullard, R.; Person, M. *Bull. Soc. Chim. Fr.* **1967**, *11*, 4115.
(35) (a) Wilke, G. *Angew. Chem.* **1960**, *72*, 581; (b) Shun, R. A. *Inorg. Synth.* **1972**, *13*, 124.
(36) Kubota, K.; Chu, B. *Biopolymers* **1983**, *22*, 1461.